# Steady State Heat Deposits Modeling in the Nb3Sn Quadrupole Magnets for the Upgrade of the LHC Inner Triplet

D. Bocian, G. Ambrosio, H. Felice, E. Barzi, R. Bossert, S. Caspi, G. Chlachidze, D. Dietderich, S. Feher, P. Ferracin, R. Hafalia, V.V. Kashikhin, M. Lamm, G.L. Sabbi, D. Turrioni, P. Wanderer, A.V. Zlobin

*Abstract*— **In hadron colliders such as the LHC, the energy deposited in the superconductors by the particles lost from the beams or coming from the collision debris may provoke quenches detrimental to the accelerator operation. In previous papers, a Network Model has been used to study the thermodynamic behavior of magnet coils and to calculate the quench levels in the LHC magnets for expected beam loss profiles. This model was subsequently used for thermal analysis and design optimization of $Nb_3Sn$ quadrupole magnets, which LARP (US LHC Accelerator Research Program) is developing for possible use in the LHC luminosity upgrade. For these new magnets, the heat transport efficiency from the coil to the helium bath needs to be determined and optimized. In this paper the study of helium cooling channels and the heat evacuation scheme are presented and discussed.**

*Index Terms*— **LHC Inner Triplet Upgrade, Quadrupole Magnets, $Nb_3Sn$ coil, Superconducting Cable Insulation, Steady State Heat Deposits, Heat Transfer.**

## I. INTRODUCTION

THE proposed luminosity upgrade of the Large Hadron Collider (LHC) at CERN [1] requires replacement of the focusing superconducting (SC) quadrupole magnets, so called "inner triplet" (IT), located at either sides of the collider interaction regions. The LARP (US LHC Accelerator Research Program) is working on the development of $Nb_3Sn$ magnet technology for particle accelerators and possible use in the LHC luminosity upgrade that involves replacing the present Nb-Ti IT quadrupoles in the two high-luminosity Interaction Regions (IR) [2].

A possible operation issue for these $Nb_3Sn$ quadrupoles is the energy deposited in the SC magnet coils by the particles coming from collision debris or lost from the beam [3]. The power dissipation in the superconducting magnet components leads to a complex process of the heat conduction and evacuation. In order to cope with this problem the study of heat transfer from the coil cables to the helium bath is required. The *Network Model* (NM) was developed to study the thermodynamic behavior of the SC coils and to calculate the quench levels of the LHC magnets for expected beam loss profiles [4]-[6]. The NM uses a well-known method, where an electrical circuit is used to model the thermal quantities. The NM was subsequently used for thermal analysis and design optimization of $Nb_3Sn$ quadrupoles. In this paper the results of steady-state analysis of US LARP $Nb_3Sn$ quadrupole magnets are presented.

Manuscript received 13 September 2011.

This work was supported by Fermi Research Alliance, LLC, under contract No. DE-AC02-07CH11359 with the U.S. Department of Energy; by the Director, Office of Science, High Energy Physics, U.S. Department of Energy under contract No. DE-AC02-05CH11231, and partially supported by the DOE through the US LHC Accelerator Research Program (LARP).

D. Bocian, G. Ambrosio, E. Barzi, R. Bossert, G. Chlachidze, S. Feher, V.V. Kashikhin, M. Lamm, D. Turrioni, A.V. Zlobin are with Fermi National Accelerator Laboratory, P.O. Box 500, Batavia, IL 60510-0500, USA (corresponding author: Dariusz Bocian; phone: +1-630-840-3299; fax: +1-630-840-3369; e-mail: bocian@fnal.gov).

S. Caspi, D. Dietderich, H. Felice, P. Ferracin, R. Hafalia, G.L. Sabbi are with Lawrence Berkeley National Lab, Berkeley, CA 94720, USA.

P. Wanderer is with Brookhaven National Laboratory, Upton, NY 11973-5000, USA.

## II. NETWORK MODEL

The *Network Model* was developed to study the thermodynamic behavior of the magnet coils and to calculate the quench levels of the superconducting magnets for typical beam loss profiles as well as to optimize heat flow paths in the new designs of superconducting magnets. The fundamental unit of the NM is the superconducting cable. The cable is subdivided in the thermal resistance elements to study the heat flow inside its structure [4]-[6]. The network model is constructed from the cable unit. In this paper a 2-dimensional Nb3Sn coil model is analyzed. The cable sample is normalized to 1 meter of cable length. Other network model elements (coil insulation, helium channels) are included in the model with a segmentation corresponding to the cable dimensions. The advantage of NM is that this model has no free tuning parameters. Only the heat conductivity of magnet components and magnet geometry is used to calculate the heat transfer in the magnet.

The values of thermal conductivities for calculating the thermal resistances of each element are taken from a commercially available database and literature [7]-[9]. Fig. 1 shows the thermal conductivity of insulation materials used in the Nb3Sn magnets analyses. The experimentally determined equation by Claudet et al. in [9] has been used for superfluid helium heat transfer calculation (1).

$$\frac{\dot{Q}}{S} = \left[\frac{X(T_c) - X(T_h)}{l}\right]^{0.29} \left[\frac{W}{cm^2}\right]$$
$$X(T) = A \cdot \left[1 - exp\left(-\left[B \cdot (2.16 - T)\right]^{2.5}\right)\right] \quad (1)$$
$$A = 520,\ B = 3$$

where:
$S$ is helium channel cross-section in [cm$^2$],
$l$ is helium channel length in [cm],
$T_c$ is the temperature of the colder channel end in [K]
$T_h$ is the temperature of the warmer channel end in [K].

This formula was determined for cylindrical channels at atmospheric pressure. In the presented calculation it is assumed that the channel shape has negligible impact on heat transfer, for lack of more adequate data. Measurements showing possible heat transfer dependence on rectangular channel shape would be useful to set proper simulation parameters.

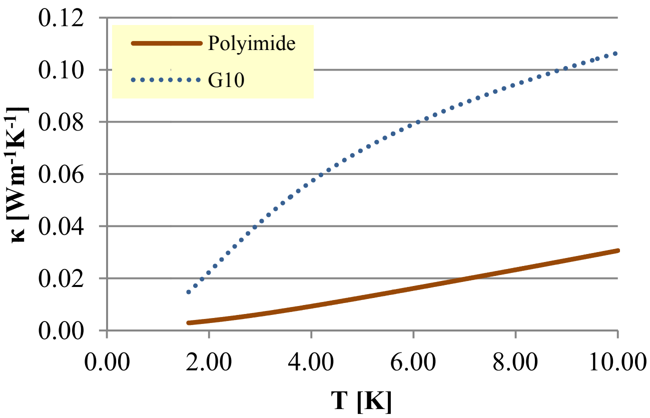


Fig. 1 Thermal conductivity of insulation materials [7].

## III. LARP $Nb_3Sn$ coil Thermal Models

The US LARP is working on the development of 120-mm $Nb_3Sn$ quadrupole magnet (HQ) [10]. The HQ coils design consists of a 2-layer cos-2θ configuration with 120 mm bore, one wedge in the inner and one wedge in the outer cable layer (Fig. 2). The HQ coil thermal network model was based on the first-generation HQ cable, which is made of 35 strands, 0.8 mm in diameter, with a nominal width of 15.15 mm, mid-thickness of 1.44 mm and keystone angle of 0.75 degree.

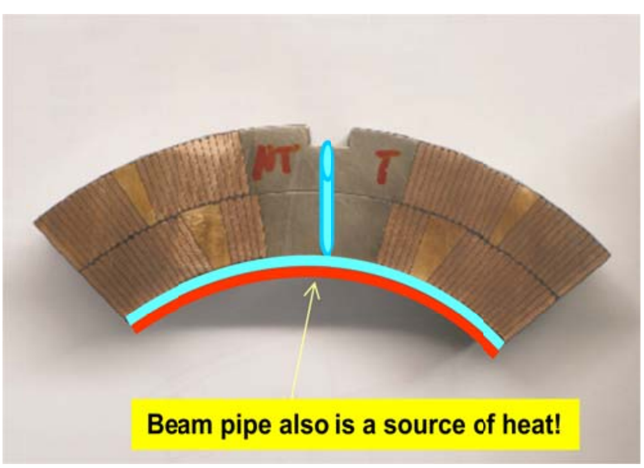


Fig. 2 A photo of HQ03 coil cross-section. A sketch of beam pipe and helium channels were added to the image in order to indicate all magnet components implemented into HQ thermal network model.

### A. Model validation

The validation of the $Nb_3Sn$ thermal Network Model was performed with data collected at Fermilab while testing a Technological Quadrupole (TQC02b) magnet at 1.9 K and 4.5 K temperatures [14]. TQ coils design consists of a 2-layer cos-2θ configuration with 90 mm bore and one wedge in the inner layer. The cable was made of 27 strands, 0.7 mm in diameter, with a nominal width of 10.05 mm, mid-thickness of 1.26 mm and keystone angle of 1.0 degree. The coils were surrounded by stainless steel collars and an iron yoke with the outer radius of 200 mm. In these measurements the LARP TQC02b was equipped with a dedicated 1-meter-long, 25.4 μm thick and 9.5-mm-wide stainless steel heating strip placed in the middle of the Kapton shim package at the coil inner layer, between adjacent coils (Fig. 3). In this location the beam induced heat deposition exhibit their maximum [14].

A thermal model including all details of TQ was developed. A vital part of the model is the heat conductivity of epoxy-impregnated S-2 glass insulation. This thermal property was approximated by the properties of fiberglass composite (G10) from [7] (Fig. 1). The heat reservoir (boundary conditions as fixed helium bath temperature) were put at the inner coil surface and the outer yoke surface, which are both in direct contact with liquid helium. It was also assumed that contribution of thermal contact resistance between different materials and between coil insulation and liquid helium is negligible with respect to the thermal resistances of coil insulation. The insulation scheme implemented into the LARP Nb3Sn magnet NM is shown in Fig. 8.

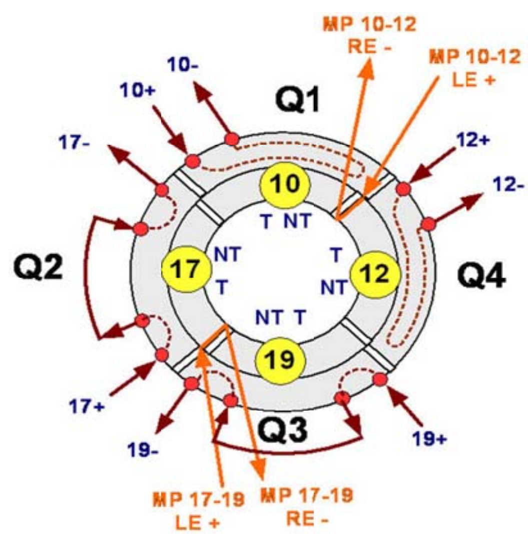


Fig. 3 The LARP Technological Quadrupole TQC02b electrical scheme. The magnet was equipped with a dedicated stainless steel heating strip placed in the inner layer mid-plane, between the adjacent coils Q1-Q4 (TQ10-TQ12) and Q2-Q3 (TQ17-TQ19).

The TQC02b was build from coils made from Modified Jelly Roll (MJR) conductor: TQ10 and TQ12, and Restacked Rod Process (RRP) conductor: TQ17 and TQ19. MJR coils had an additional layer of 43 μm inner polyimide (kapton) trace. The cables used in these coils (RRP and MJR) were insulated with S-2 glass sleeves. After winding and high-temperature reaction, the coils were impregnated with epoxy resin. The thickness of insulation and epoxy in the final coil depends on the type of insulation and the pressures during reaction and impregnation. The thickness may differ from the nominal, raising large uncertainties in magnet quench limit under the beam induced heat depositions in the coil. In order to set correct data in the model the actual insulation thickness of the RRP and MJR coils used in TQC02b were measured (TABLE 1).

The experimental setup, consisting of a dedicated heating strip and DC power supply, enabled provoking quenches at magnet current in the range of from a few hundreds to about 9000 amperes. Each measurement involved setting the heater current to a chosen value, waiting for a few minutes to establish steady-state heat flow, and then ramp the magnet current to quench at 20 A/s in order to avoid additional coil heating by eddy currents.

Fig. 4 shows the calculated and measured quench currents of the inner mid-plane cable. The calculated quench performance is linear in the whole data range. There is a good correlation between the calculated and measured values both at 1.9 K and 4.5 K temperatures for both RRP and MJR coils. The discrepancy for low quench current values, involving higher conductor temperature suggest non-linear dependence of critical current density on temperature, recently confirmed by NIST measurement of RRP 54/61 strands [15]. Unfortunately, $J_c$(T) results for MJR conductor are not available.

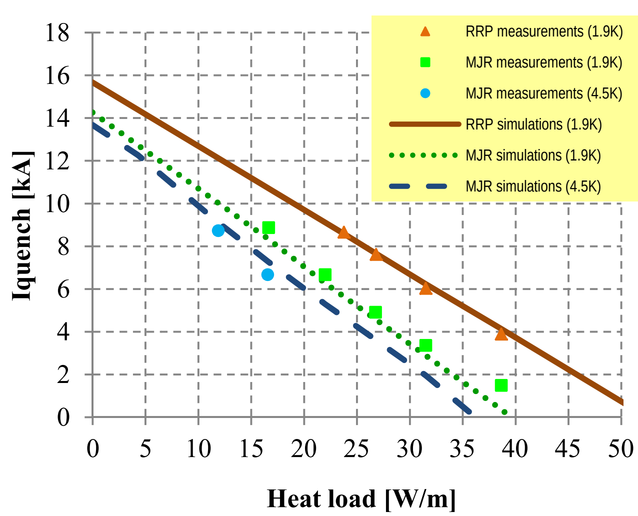


Fig. 4 TQC02b thermal model validation with measurements. Solid line and triangle markers show results of simulation and measurements at 1.9 K for RRP coils. Dotted line and square markers corresponds to measurements taken at 1.9 K with MJR coils. Dashed line and round makers corresponds to measurements taken at 4.5 K with MJR coils.

### B. HQ Magnet Numerical Simulations

The NM was used for thermal analysis and design optimization of HQ $Nb_3Sn$ quadrupole for the typical beam induced heat load (Fig. 5). The HQ thermal model included all the features of the $Nb_3Sn$ coil and implemented insulation scheme (Fig. 8) is listed in TABLE 1.

Different inner coil insulation schemes have been studied in order to understand their impact on the thermal coil behavior. Also helium channels dimensions i.e. annular helium channel between coil and cold bore, and helium channels through coil poles, were studied in details in order to efficiently evacuate heat from the HQ coils and to keep the helium in the channels in superfluid regime. The helium channel was dimensioned in order to simulate holes with 5 mm diameter set every 100 mm along the coil. The holes diameter was decided in order to have the channels in the poles equal or larger than annular channel cross-section (avoiding helium quench in the pole channels).

The heat load profile for LHC IT upgrade layout is not available, yet. An estimated heat load profile at $L=5*10^{34}$ cm$^{-2}$s$^{-1}$ has been used in order to study qualitative different inner coil insulation schemes as well as coil cooling channels. The transverse heat deposition profiles implemented into HQ model is shown in Fig. 5. This profile was obtained from MARS [17]-[18] simulation performed for a phase I upgrade LHC IP5 optics layout [19]. The MARS model included beam screen, beam tube and annular cooling channel. In order to reduce the heat loads in the magnet mid-plane an additional 3 mm tungsten absorber in the horizontal and vertical planes was added in the simulations. An interpolation algorithm was run on the MARS output in order to fit the MARS heat load map to the HQ coil conductor map. Also heat load in the cold bore was implemented into the model in order to study the efficiency of annular cooling channel between the cold bore and the inner surface of the coil.

The results of HQ NM simulations are shown in Fig. 6 and Fig. 7 for the inner and outer cable layer respectively. Zero in this figures indicate the magnet mid-plane, positive and negative x-values indicate cables in the coils part adjacent to the mid-plane and y-values indicate temperature increase in the cables above bath temperature $T_0$=1.9 K for the heat load shown in Fig. 5. Three scenarios were studied and shown in this figure: 1) only cable insulation in coil inner diameter (ID), 2) cable insulation + additional 127 µm G10 insulation layer in ID, 3) cable insulation + additional 127 µm G10 and 43 µm polyimide insulation layer in ID. The non-symmetric temperatures distributions coming from the fact that heat load is not symmetric.

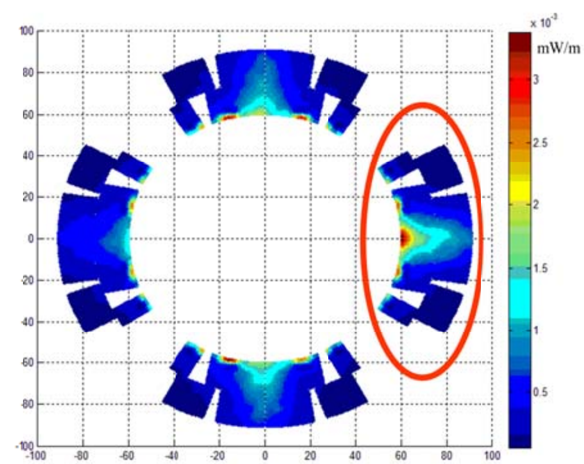


Fig. 5 The transverse heat deposition profiles implemented into HQ thermal model. This profiles was obtained from MARS simulation performed for an upgraded LHC IP5 optics layout for $L=2.5*10^{34}$ cm$^{-2}$s$^{-1}$. In the thermal simulation this heat load multiplied by a factor 2 was used in order to get results for nominal LHC upgrade luminosity ($L=5.0*10^{34}$ cm$^{-2}$s$^{-1}$). The heat load on the right quadrant was implemented in the NM.

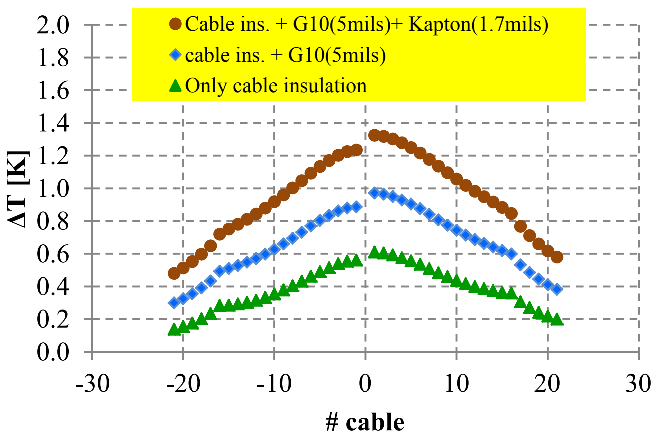


Fig. 6 Results of the numeric simulation – HQ inner cable layer. Zero in this figure indicate magnet mid-plane, positive and negative x-values indicate cables in the coils part adjacent to the mid-plane and y-values indicate temperature increase in the cables above bath temperature $T_0$=1.9K for the heat load shown in Fig. 5.

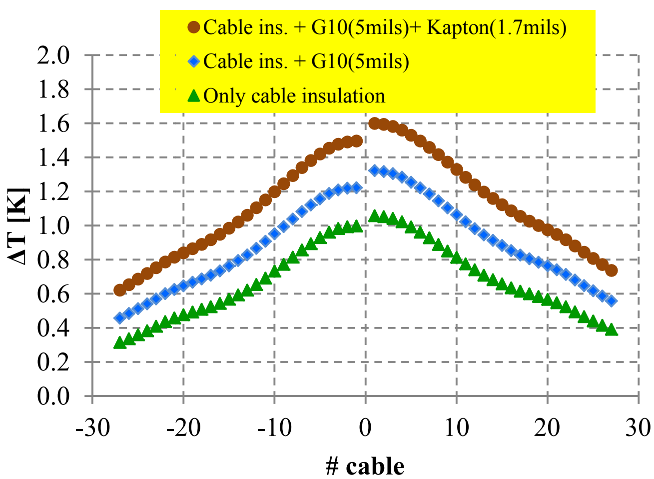


Fig. 7 Results of the numeric simulation – HQ outer cable layer.

## IV. Conclusion

A Network Model was used to simulate the thermal behavior of $Nb_3Sn$ magnets and was successfully validated with experimental data. The calculated and measured data are in good agreement and validates the model accuracy, the material properties used in simulations and also verifying choice of boundary conditions.

A 120 mm US LARP $Nb_3Sn$ magnet was analyzed with this model. An estimated heat load distribution at luminosity $L=5.0\cdot10^{34}cm^{-2}s^{-1}$ was implemented in order to qualitative study the coil insulation as well as magnet helium channels cooling efficiency. The results show significant temperature increase in the coil due to increasing of inner coil insulation thickness. In order to efficiently evacuate heat from the coil the polyimide insulation should be minimized. The proposed helium channel dimensions ensure helium keep in superfluid regime.

The thermal studies of $Nb_3Sn$ magnets will continue using refined heat load maps, updated magnet designs and IT layout.

## V. Appendix

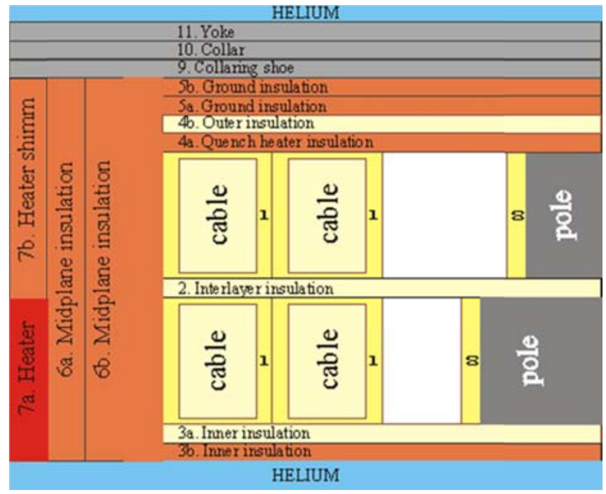


**Fig. 8** TQC02b coil insulation scheme and heating strip implemented into network model.

**TABLE 1** TQ and HQ coils insulation scheme implemented in the NM. The difference of TQ cable and coil insulation thickness was observed in MJR and RRP type coils. A nominal insulation scheme was implemented in the HQ thermal model (last column).

| **Item** | **Material** | **MJR (TQ 10-12)** | **RRP (TQ 17-19)** | **RRP HQ coil** |
|---|---|---|---|---|
| | | thickness [μm] | thickness [μm] | thickness [μm] |
| 1 | S-2+epoxy | 99 | 95 | 127 |
| 2 | S-2+epoxy | 327 | 165 | 254 |
| 3a | Kapton | 43 | 0 | 76 |
| 3b | S-2+epoxy | 299 | 208 | 127 |
| 4a | Kapton | 43 | 43 | 76 |
| 4b | S-2 +epoxy | 273 | 165 | 381 |
| 5a | Kapton | 127 | 127 | 127 |
| 5b | Kapton | 127 | 127 | 127 |
| 6a | Kapton | 76.2 | 76.2 | 127 |
| 6b | Kapton | 50.8 | 50.8 | - |
| 7a | Stainless steel | 25.4 | 25.4 | - |
| 7b | Kapton | 25.4 | 25.4 | - |
| 8 | S-2+epoxy | 76.2 | 76.2 | 127 |
| 9 | Stainless steel | 787.4 | 787.4 | 787.4 |


## Acknowledgment

The main author would like to thank people who helped during the course of this work: N. Cheggour, A. Ghosh, F.L. Goodrich, E. Todesco and D. Tommasini.

## REFERENCES


[1] LHC Design Report, The LHC main ring, vol. 1, CERN-2004-003.
[2] J. B. Strait *et al.*, “Towards a new LHC interaction region design for a luminosity upgrade,” in *Proc. 2003 Particle Accel. Conf.*, pp. 42–44.
[3] R. Schmidt et al., “Beam loss scenarios and strategies for machine protection at the LHC”, *LHC Project Report 665*, CERN, 2003.
[4] D. Bocian, B. Dehning, A. Siemko, “ Modeling of quench limit for steady state heat deposits in LHC magnets”, IEEE Appl. Trans. Supercond., 18 (2008) 112-115.
[5] D. Bocian, B. Dehning, A. Siemko, “Quench Limit Model and Measurements for Steady State Heat Deposits in LHC Magnets”, IEEE Trans. Appl. Supercond. 19 (2009) 2446-2449
[6] R. Bruce, D. Bocian, S. Gilardoni and J. M. Jowett, “Beam losses from ultraperipheral nuclear collisions between $^{208}Pb^{82+}$ ions in the Large Hadron Collider and their alleviation, Phys. Rev. ST Accel. Beams 12, 071002 (2009)
[7] Cryosoft, France, 2001.
[8] S.W. Van Sciver, Helium Cryogenics, Plenum Press, New York, 1986.
[9] Claudet et al., CRYOGENIE et ses applications en supraconductivite, IIF/IIR
[10] H. Felice et al., “Design of HQ – a High Field Large Bore $Nb_3Sn$ Quadrupole Magnet for LARP”, *IEEE Trans. Appl. Supercond.*, vol. 19, no. 3, June 2009, pp 1235-1239.
[11] A. V. Zlobin et al., “Large-aperture $Nb_3Sn$ quadrupoles for 2nd generation LHC IRs,” in Proc. 2002 European Particle Accel. Conf., Paris, France, pp. 2451–2453.
[12] I. Novitski, A.V. Zlobin, “Thermal analysis of SC quadrupoles in accelerator interaction regions,” IEEE Trans. Appl. Supercond., vol. 17, no. 2, pp. 1059–1062, Jun. 2007.
[13] R.C. Bossert *et al.*, “Fabrication and test of LARP technological quadrupole models of TQC series,” *IEEE Trans. Appl. Supercond.*, vol. 19, no. 3, Jun. 2009.
[14] V.V. Kashikhin et al., “Quench margin measurement in $Nb_3Sn$ quadrupole magnet”, *IEEE Trans. Appl. Supercond.*, vol. 19, no. 3, Jun. 2009.
[15] private communication: N. Cheggour (najib.cheggour@nist.gov), F.L. Goodrich (loren.goodrich@nist.gov),
[16] V.V. Kashikhin, N. Mokhov, et al., „Performance of $Nb_3Sn$ quadrupole magnet under localized thermal load”, Fermilab-conf-09-316-TDN.
[17] N.V. Mokhov, http://www-ap.fnal.gov/MARS/
[18] N.V. Mokhov, Rakhno I.L., Kerby J.S., Strait J.B., “Protecting LHC IP1/IP5 Components against Radiation Resulting from Colliding Beam Interactions”, Fermilab-FN-732 (2003), LHC Project Report 633.
[19] J. A. Johnstone et al.,”Optics implications of implementing $Nb_3Sn$ magnets in the LHC phase I upgrade”, *Proc. 2008 European Particle Assel. Conf.*, pp. 2626-2628.